Comparative Study of Micro-nozzle characteristics under marginally rarefied and continuum treatments

Athrva Atul Pandhare,[1] Abhishek Puri,[1] and S. Senthilkumar[1]
Department of Aerospace Engineering, SRM Institute of Science and Technology, Kattankulathur, Tamil Nadu 603203, India

It is generally accepted that, for a micro-channel flow, the necessity of applying slip boundary conditions occurs when Kn>0.01. These special boundary conditions are required to resolve the transition from no-slip to partial slip at the walls. This paper presents a comparative study between the results obtained after applying such special boundary conditions(first-order slip formulation) and the results obtained without applying any conditions (No-Slip). The purpose of doing so is to see whether the increase in Knudsen number corresponding to a marginal rarefied flow, necessitates the application of special boundary conditions. Furthermore, an attempt is made in this paper to see whether a significant change occurs in nozzle performance characteristics like thrust, exit pressure and exit velocity magnitude due to the change in flow regime. Such comparative studies are conducted for both, conical and bell nozzles whose diameters vary from 30μm to 40000μm. The slip formulation is applied using a UDF function.

I. INTRODUCTION

A nozzle is a component that is extremely important in the design of any propulsion system. Micro-Nozzles have a throat diameter ranging in micrometres and may even tend to smaller values. Although the velocities attained in micro-nozzles are appreciable, the resulting Reynolds number at the throat of such nozzles is a comparatively small value from Re 10^1 to 10^3 .The result of this is that viscous effects cannot be ignored and a inviscid treatment is flawed.[5]

Low Reynolds number flow, when coupled with the possible high Knudsen number may result in flow departing from the continuum regime. There exists the thermo-fluidic complexity of a supersonic flow in tandem with subsonic viscous boundary layers that extend from the walls. At these low Reynolds numbers it is possible that the viscous layer occupy a sizable fraction of the divergent nozzle cross-section and, consequently, impact the performance of the nozzle[10]. There is also the effect of heat transfer, which is more pronounced due to the high surface area- volume ratio in micro-nozzles. Furthermore, it is observed that high Knudsen numbers tend to depart the flow regime towards rarefied and free molecular flow. As a result the ensuing flow may have distinct regions of applicability of the continuum treatment, and rarefied or free molecular treatments[10]. It is important that the above discussed points be accounted for in the development of micro-nozzles. For the same reasons an analysis of the flow in the micro-nozzles is necessarily computational, and it gives us a better understanding of the underlying physics. Various studies have been conducted to assess the performance of micro-nozzles, and the computational models used in their study. Some of the more relevant studies are mentioned here. Grm et al.[5] have used the finite Volume moving boundary method to obtain an estimate of wall slip velocity. The base mathematical model used is the Navier- Stokes Fourier partial differential equations for the description of compressible gases. The propellant used is pure nitrogen gas[5]. The criterion used by the group of researchers to mark a change in flow regime, is the local Knudsen number. It was suggested in the paper that a coupled solver be used wherein a Navier-Stokes model is used for the convergent side of the nozzle and a molecular model is used for the aft part (divergent section) where the flow departs from continuum treatment. Ranjan et al.[9] have used an experimental setup was for a cold gas micro-thruster. The micro-nozzle used here has dimensions in the range of a few micro-meters. The gas used was compressed air, at $300K$. The computational results were validated by experimental results, the tests were conducted in vacuum and sea level environment. A Planar micro-nozzle was fabricated in the form of a chip. The paper indicates that the preferable semi-divergent angle should be 28 degrees and the expansion ratio must be in the range $20-400$. The expansion ratio used however, is 15 due to design and fabrication constraints. The results were obtained for a pressure difference (ΔP) of $1-4$ bar[9]. Furthermore the work done by Xie et al.[10] also provides some insight in the problem under consideration. In this paper, 2- D micro-nozzle analysis was conducted, it was indicated that a two dimensional reduction of planar micro-nozzles is appropriate when the width-to-height ratio is large. Furthermore, it was concluded that the mass flux would increase by 3% in a 2-D case as compared to a 3-D case. The paper also compared results from DSMC based simulations and Navier-Stokes based simulations of the same nozzles. Furthermore, it was also concluded that DSMC yielded results that were on an average $2-4\%$ higher on the whole range of pressure difference than experimental results and Navier-Stokes based models yielded results that were $1-3\%$ lower than the experimental results. This indicates that Navier – Stokes based slip conditions are appropriate for getting good estimations for wall slip velocity and work well in resolving the behavior of marginally rarefied flow regime. Additionally some motivation was derived from the work of W.F. Louisos et al.[8], wherein, 2-D numerical simulations for the micro-nozzle design of NASA/GSFC prototype microthruster were conducted. The study was mainly aimed at illustrating the impact of viscous forces on performance. For Reynolds number $Re < 1000$, nozzles of different semi- divergent angles were studied under adiabatic conditions. It was observed that a reduction in thrust took place as the semi-divergent angle was increased above 30 degrees. It was also found that for a H_2O_2 based nozzle the optimum angle was 30 degrees. While for N_2H_4 based micro-nozzles, no distinct maximum thrust output

was recorded that corresponded to an optimal geometry. The most effective half- angle in this case was <25 degrees. Finally, In the work done by Darbandi et al.[11], micro-nozzle analysis was conducted using an unstructured DSMC solver and the results were compared with Navier – Stokes based first order slip conditions for rarefied flow. The gas used was Nitrogen. The plots for Wall slip velocity and temperature jump were plotted. It was found that the results produced by the DSMC and Navier- Stokes based models were generally in agreement with each other. The boundary conditions were : $P_{in} = 1$ bar, $T_{wall} = 300K$, $D_{throat} = 30$ μm. In the nozzles presented in this paper, a comparative study is conducted between the continuum treatment and the marginally-rarefied treatment of micro-nozzles. This is conducted to establish the effects of the above mentioned treatments in the characteristic properties of the nozzles (i.e. thrust). Furthermore by varying the characteristic length(diameter) of the micro-nozzles, the physical dimensions at which the application of special slip boundary conditions becomes necessary, can also be found. It is also important to understand whether the nozzle geometry affects the wall slip velocity and temperature jump, for this purpose conical and bell nozzles of similar dimensions are compared.

II. SIGNIFICANCE OF KNUDSEN NUMBER

The condition of no- slip, which translates to the notion that the velocity of any flow near a wall is equal to the velocity of the wall is inexact. The kinetic theory of gases predicts a finite velocity of slip at a wall. This velocity becomes important as the characteristic length approaches the mean free path of molecules.

The Knudsen number(Kn) is a dimensionless quantity that is defined as the ratio of mean free path to the characteristic length of a fluid. This number is used to mark a transition between different regimes of flow. For instance, it is generally accepted that *Continuum regime* of flow can be used for all flow problems where the $Kn < 0.001$[11] and afterward special formulations accounting for *'non-continuum'* effects must be used.

A general expression for Knudsen number is,

$$Kn = \frac{\lambda}{L} \tag{1}$$

Here, λ is the mean free path of the fluid molecules, and L is the characteristic length of micro-nozzle. A simplified version of the above equation includes terms of Mach number (M), Reynolds number (Re), and specific heat ratio (γ) and can be written as,

$$Kn = \sqrt{\frac{\gamma\pi}{2}}\frac{M}{Re} \tag{2}$$

Since the Knudsen number marks a transition between different regimes of flow, it shows up in the special formulations for implementing slip on walls of the nozzle.

III. MATHEMATICAL MODELS

The governing equations for micro-nozzle flow field are the compressible Navier-Stokes equations which have been solved using an implicit solver for all simulations. The governing conservation equations for mass, momentum, and energy are[5],

$$\frac{\partial \rho}{\partial t} + \nabla.(\rho V) = 0 \tag{3}$$

$$\frac{\partial (\rho V)}{\partial t} + \nabla.(\rho V \otimes V) = -\nabla.(p) + \nabla.(\tau) \tag{4}$$

$$\frac{\partial (E)}{\partial t} + \nabla.((\rho E + p)V) = \nabla.(k(T)\nabla(T) + (\tau.V)) \tag{5}$$

$$E = h - \frac{p}{\rho} + \frac{V.V}{2} \tag{6}$$

$$\tau = \mu(T)\left((\nabla V + \nabla V^{\mathrm{T}}) - \frac{2}{3}\nabla.VI\right) \tag{7}$$

The above system of equations is closed by the Ideal Gas Equation. In these equations, ρ is the density, V is the velocity, t denotes the time, E is the specific energy, and p is the absolute local pressure, μ is the fluid viscosity, k is the thermal conductivity, T is the static temperature, h is the enthalpy, and τ is the viscous stress tensor.

A. MATHEMATICAL MODEL FOR ACCOMMODATING TRANSITION TO RAREFIED REGIME

The first order slip formulation has been used to impose partial slip to the divergent wall of the micro-nozzle.[11]

$$u_g - u_w = \frac{2-\sigma_u}{\sigma_u} Kn \frac{\partial u}{\partial n} \tag{8}$$

$$T_g - T_w = \frac{2-\sigma_T}{\sigma_T}\left(\frac{2\gamma}{\gamma+1}\right)\left(\frac{Kn}{Pr}\right)\frac{\partial T}{\partial n} \tag{9}$$

In the above equations, u_g is the slip velocity of the gas. u_w denotes the velocity of the wall where fluid slip takes place, this velocity is only applicable in the case of a moving wall. σ_u denotes the momentum accommodation coefficient, which is unity in our case[11].T_g is the temperature of the gas in the cell thread that is adjacent to the wall,T_w is the wall temperature. σ_T denotes the thermal accommodation coefficient whose value is also unity[11]. Kn is the Knudsen number and Pr is the Prandtl number.

IV. DESIGN CONSIDERATIONS

A conical nozzle was selected having a expansion ratio of 4.667[11] this nozzle was used for validations, the following equations were used for the the design of the bell nozzle. The detailed procedure for design of bell nozzle is as follows:
First expansion ratio is fixed, then the exit-to-chamber pressure ratio is calculated from the expansion ratio. A 2-D Design of the nozzle is shown in Figure 1 where R_t is the throat radius, R_e is the exit radius, ε is the expansion ratio. L_n is the length of the nozzle's divergent portion, α is the semi- divergent angle and finally, θ_n and θ_e are the initial and final wall angles.
The equations employed for this are as shown[7]:

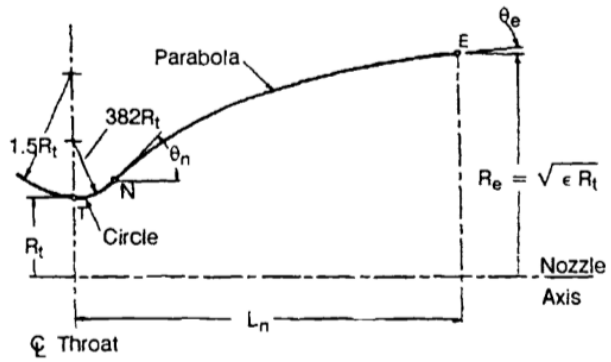

FIG. 1. Bell Nozzle Design[7]

$$(\delta)^{(2/\gamma)} - (\delta)^{(\gamma+1)/\gamma} = \left(\frac{1}{\varepsilon^2}\right)\left(\frac{\gamma-1}{\gamma+1}\right)\left(\frac{2}{\gamma+1}\right)^{2/(\gamma-1)} \tag{10}$$

where δ is the ratio $\frac{P_e}{P_c}$ called the exit-chamber pressure ratio, P_e is the exit pressure and P_c is the chamber pressure. Once the exit-chamber pressure ratio is obtained, the Coefficient of thrust C_f is calculated by the following expression.

$$C_f = \sqrt{\frac{2\gamma^2}{\gamma-1}\cdot\frac{2}{\gamma+1}^{\frac{(\gamma+1)}{\gamma-1}}\left(1-\frac{P_e}{P_c}^{\frac{\gamma-1}{\gamma}}\right)+\left(\frac{P_e}{P_c}-\frac{P_a}{P_c}\right)\left(\frac{A_e}{A_t}\right)} \tag{11}$$

Where P_a is the ambient Pressure. The above value of C_f was not corrected for viscous effects. Further, knowing the thrust to be produced, the throat area was found by the equation,

$$F = C_f P_c A_t \tag{12}$$

The Chamber pressure was assumed to be 1 bar. From the throat area A_t the throat diameter was calculated d_t. Having a value of the chamber pressure P_c and the ratio δ an average value of the exit pressure P_e was calculated. The mass flow rate can be calculated from,

$$\dot{m} = \frac{P_c A^\star}{\sqrt{T_c}}\sqrt{\left(\frac{\gamma}{R}\right)\frac{2}{\gamma+1}^{\frac{\gamma+1}{\gamma-1}}} \tag{13}$$

where R is the gas constant, T_c is the chamber temperature, and *gamma* is the ratio of specific heats. It should be noted that the above calculation does not account for the viscous decrease in the value of C_f, further it also ignores the coefficient of discharge C_d of the nozzle in the calculation of the mass flow rate.
The Exhaust velocity (V_j) is given by,

$$V_j = \sqrt{\frac{2\gamma RT_c}{\gamma-1}\left(1-\frac{P_e}{P_c}\right)^{\frac{\gamma-1}{\gamma}}} \tag{14}$$

The expansion ratio of the bell nozzle was kept equal to the conical nozzles.

A. Mesh Independence

All the simulations are carried out with structured meshes as shown in Figure 2. Three different cases were simulated with different number of elements to check for mesh Independence.The velocity at outlet was compared in all the cases. For accurate results the elements size near the throat diameter

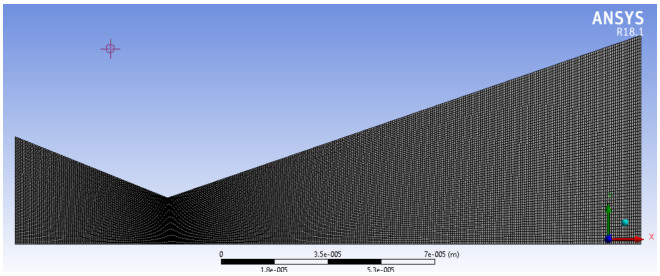

FIG. 2. Mesh

should be small. Table 1 shows different mesh configurations used to establish mesh independence. No significant changes in the results were observed, hence, for all the simulations 25000 elements was fixed.

TABLE I. Number of element VS Velocity in outlet

Number of element & Average Velocity(m/s)
21892 & 542
40705 & 542
70433 & 542

V. NUMERICAL SCHEME

An Implicit solver has been used for all the simulations. Laminar model has been used throughout, because the Reynolds number in the nozzle domain was sufficiently small. The main reason for this is the small characteristic length of the nozzle (in micro-meters) which was comparable to the mean free path of the molecules of the fluid. This behaviour is fundamentally different from *macro-nozzles*, where

the Reynolds numbers are high owing to high flow velocities and large characteristic lengths.

A. Choice of fluid and properties

The fluid that was used for all the simulations was pure Nitrogen. Nitrogen was chosen for the following reasons:
1. Condensation temperature of Nitrogen is very low and hence it cannot undergo a phase change in the interior or the exhaust of the nozzle.
2. Nitrogen is a commonly used fluid in micro-nozzles and a lot of literature has been found on it, making validation easier and more reliable.
Table 2 illustrates the property wise models used for nitrogen

TABLE II. Property Table

Property & Model
Density & Ideal gas
Specific heat(constant pressure) &Polynomial
Thermal Conductivity &Polynomial
Viscosity &3 coefficient Sutherland
Molecular weight &Constant

B. Application of Partial Slip

It is important to apply a special mathematical condition for modelling partial slip as is generally accepted for transitional flows. For this reason first order slip condition has been applied at the wall of the nozzle[11]. Temperature jump has also been modelled at the walls of the nozzle. These boundary conditions have been shown[11][10] to produce sufficiently accurate results.
The application of the boundary conditions has been accomplished using a UDF (User Defined Function), the flow solver uses Navier-Stokes equations and the commercial software used is ANSYS fluent.

VI. VALIDATION

Validation is required to establish a working computational model. For this reason, the results produced by previous literature have been reproduced using the developed UDF code. Since the work done by [11] seems the most relevant to our study, it was used for validation. The results shown compare the temperature jump and wall velocity profile in [11] with our UDF.
Figure 3 depicts the comparison between temperature jump profiles. It is conspicuous that there exists a good agreement between the two results. It can be seen that there is a drop in temperature (thermal discontinuity), as is expected. There are two pronounced dips in the temperature which are observed at the nozzle throat and the nozzle exit. It is hypothesised that this occurs due to the rapid expansion of the fluid at these

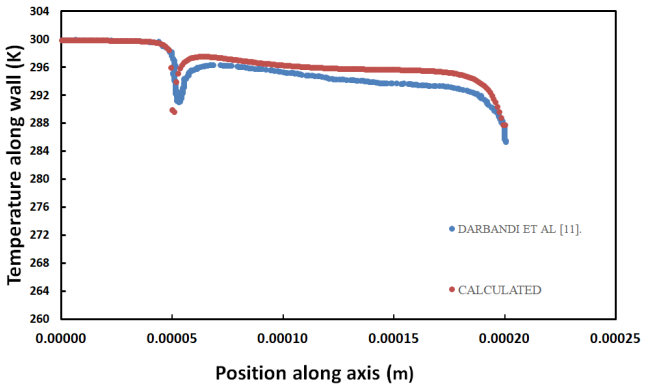

FIG. 3. Temperature Jump Profile Validation

points. It should be noted that the nozzle design used has no fillet at the throat to allow for gradual expansion. This translates to higher values of temperature gradients. Since thermal jump varies in direct proportion to temperature gradients, it is observed that a greater temperature discontinuity exists here.
The same behavior can be observed in the wall slip velocity profile, as shown in Figure 4, two pronounced peaks in the slip velocity are observed, first, at the throat and the latter at the nozzle exit. The reason for such an occurrence is that there exist large velocity gradients at these points (due to rapid velocity increase owing to expansion). A higher peak is observed at the exit of the nozzle, because the gas exits into free space here.

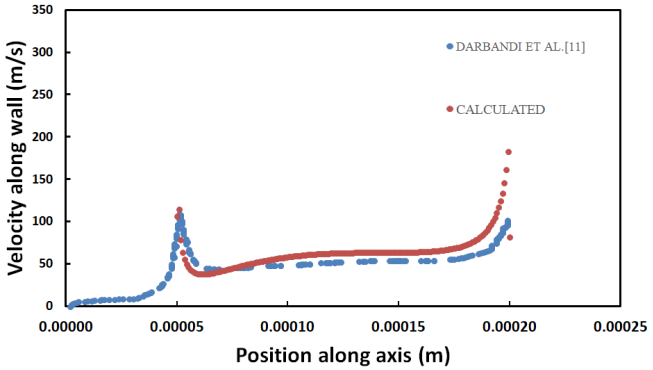

FIG. 4. Wall Velocity Profile Validation

Thus the results obtained were found to agree well with previous work and preserve the physicality of the expected phenomena.

VII. RESULTS AND DISCUSSION

This section enumerates the results and provides a brief explanation of the trends seen. A number of nozzles have been simulated, each nozzle having a different throat diameter by

Keeping the expansion ratio fixed. Wall slip velocity and thermal jump profiles have been plotted and compared. This can be used to study the general pattern of the slip characteristics with a decreasing throat diameter.

A. Wall Slip Velocity : Profile and Discussion

1. *Conical Nozzles*

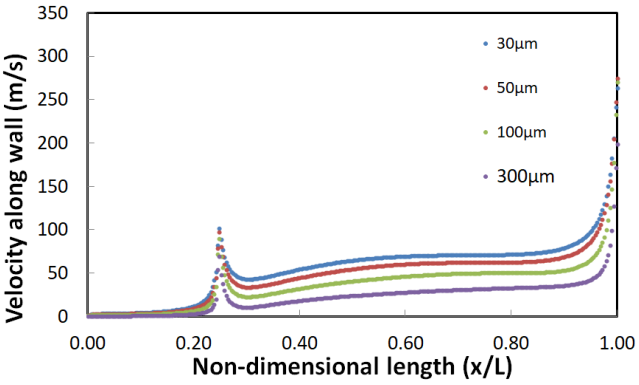

FIG. 5. Wall Velocity Profiles for varying throat diameters

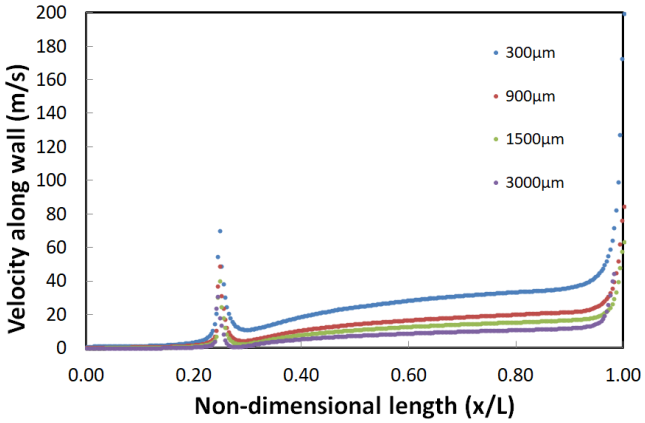

FIG. 6. Wall Velocity Profiles for varying throat diameters

Figure 5-6 show the wall slip velocity profile for nozzles with throat diameter varying from $3000\mu m$ to $30\mu m$. It can be seen that, for the smallest throat diameter, the wall slip velocity recorded was maximum, as the throat diameter is increased, the wall slip velocity decreases. This trend is expected, because as the nozzle dimensions are decreased, the Knudsen numbers reached in the nozzle increase, marking a stronger departure from continuum regime. Figure 7 depicts an overall trend that relates the characteristic length and the slip velocity reached in the nozzle. It can be seen that the slip velocity is higher for smaller diameter nozzles than for

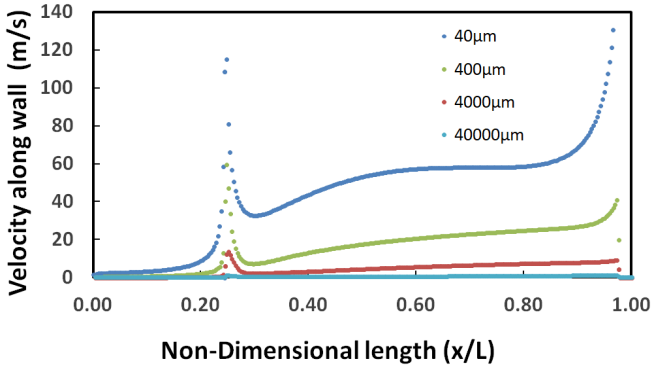

FIG. 7. Wall Velocity Profiles for varying throat diameters

larger diameter nozzles. Simulations were carried for nozzles of higher throat diameters, up to $D_{throat} = 40000\mu m$. It was observed that the slip velocity decreased and almost became negligible for $D_{throat} = 40000\mu m$ at which point the simulations were stopped, as this may indicate a complete transition from the marginally rarefied (transition) to continuum regime.

2. *Bell Nozzle*

An Identical study to the one shown above was carried out for Bell nozzles. The results obtained are shown as follows.

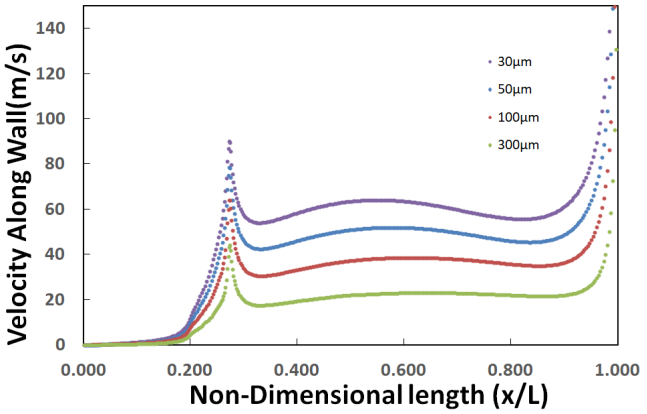

FIG. 8. Wall Velocity Profiles for varying throat diameters

Figure 8-9 depict the wall slip velocity for bell nozzles with diameters ranging from $30\mu m$ to $3000\mu m$.
On an average, it was seen that the peak slip-velocity reached at the nozzle throat was higher in case of conical nozzles than bell nozzles. This is because the bell nozzle used in this study allows for a gradual expansion of the fluid, in turn decreasing the magnitude of temperature and velocity gradients. The peak slip velocity reached at the exit depends on the exit pressure and the design of the nozzle (An under-expanded nozzle is expected to produce a higher peak slip velocity due to rapid expansion at the exit). The peak wall slip velocity at the exit

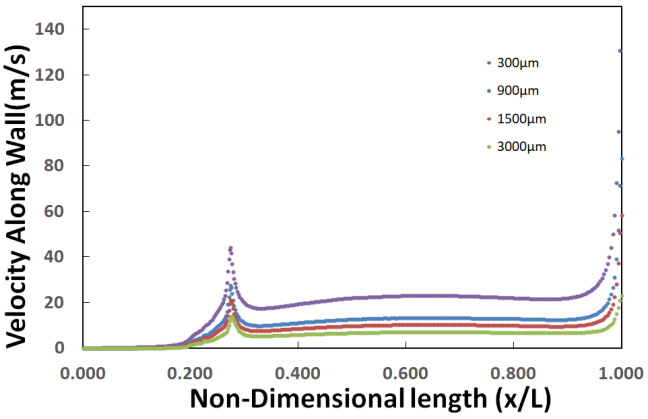

FIG. 9. Wall Velocity Profiles for varying throat diameters

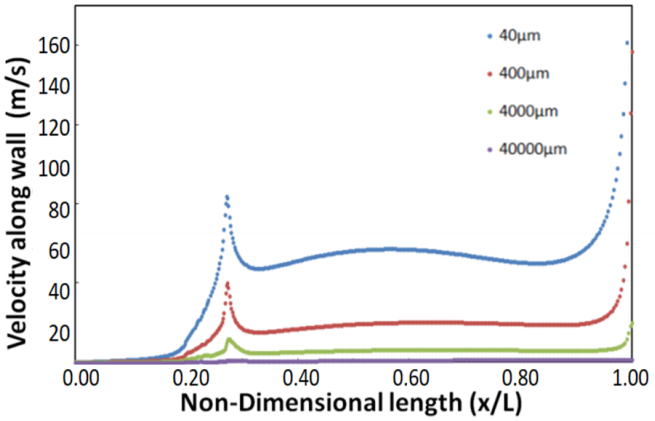

FIG. 10. Wall Velocity Profiles for varying throat diameters

may not always be controlled, because, for nozzles operating in a vacuum, the design cannot be made to allow for optimal expansion under all conditions.
Finally, Figure 10 reinforces the fact that a larger diameter implies a smaller Slip velocity and vice versa.

B. Temperature jump: Temperature Discontinuity

1. *Conical Nozzle*

Temperature jump profiles for nozzles with different throat diameters was plotted. Figure 11 depicts the temperature jump profile for different nozzles. It is apparent that the temperature discontinuity at the wall ceases to exist at larger throat diameters. The nozzle with 40000μm throat diameter shows almost no temperature jump along the wall. Furthermore, the temperature jump profile even at 40μm is of a small magnitude (order of a few Kelvins).

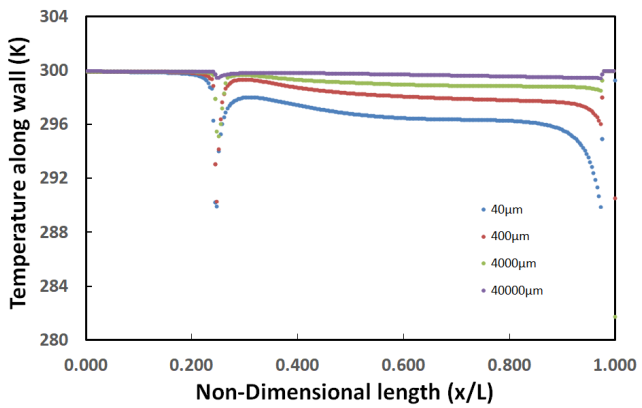

FIG. 11. Temperature jump profiles for varying throat diameters

2. *Bell Nozzle*

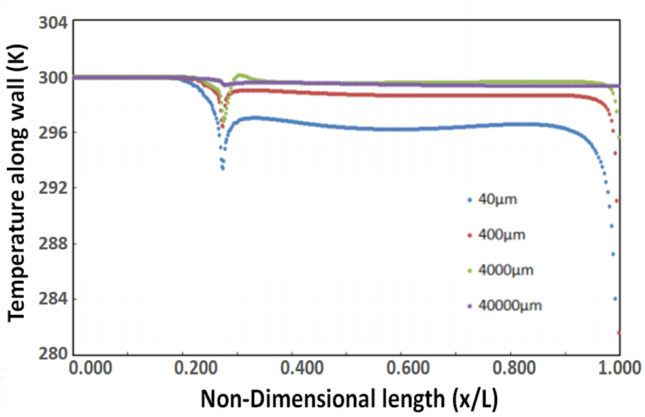

FIG. 12. Temperature jump profiles for varying throat diameters

Figure 12 illustrates the temperature jump phenomenon as observed in bell nozzles. It was seen that the temperature discontinuity was maximum at the nozzle throat and at nozzle exit(seen as two prominent dips in the plot). This is due to the rapid expansion of the fluid at these two locations that facilitates rapid cooling. It was observed that the temperature jump, on an average was similar in both conical and bell nozzles.

VIII. COMPARISON BETWEEN SLIP AND NO-SLIP

A. Conical Nozzles

In this section the characteristics of the nozzles(conical and bell) are assessed under slip and no-slip treatments and the differences if any are highlighted. The properties used for comparison are, thrust, exit pressure,exit velocity, mass flow rate.

1. Thrust : Percentage Difference

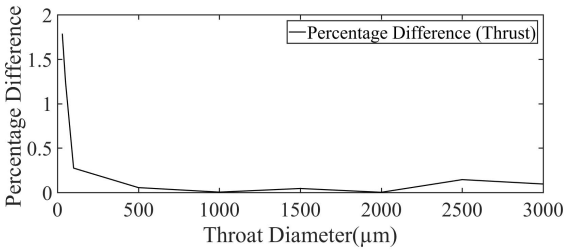

FIG. 13. Conical Nozzle : Thrust percentage difference

It can be seen from Figure 13 that the difference between the thrust values obtained by applying the slip and the no-slip treatments is very small. The maximum percentage difference is obtained for the $D_{throat} = 30\mu m$. This is an expected result because the Knudsen number in the interior of this nozzle is tending to the marginally rarefied regime. Furthermore, It should be kept in mind that as one begins to consider nozzles of $D_{throat} \leq 30\mu m$, the difference increases and the application of slip formulations become necessary.

2. Mass Flow Rate : Percentage Difference

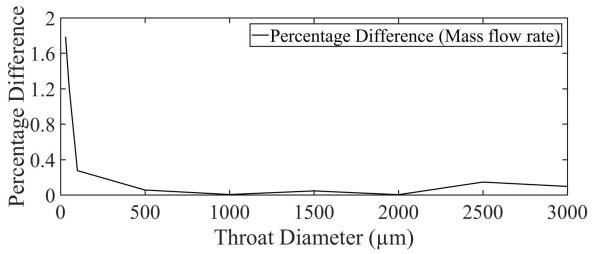

FIG. 14. Conical Nozzle : Mass flow rate percentage difference

A similar trend is seen in Figure 14 for mass flow rate. The difference in mass flow rate as obtained for these nozzles is negligible and the maximum values the percentage difference of mass flow rate is $\approx 1.1\%$.

3. Velocity Magnitude : Percentage Difference

Furthermore, the percentage difference in the exhaust velocity from the nozzle is plotted for the complete range of conical nozzle diameters and a similar trend is visible. This is illustrated in Figure 15

4. Exit Pressure : Percentage Difference

Finally, Figure 16 shows the percentage difference of Exit pressure(P_e) values under the slip and no-slip treatments. Results obtained suggest that the percentage pressure difference between slip and no-slip treatments for nozzle of $D_{throat} \in \{30, 3000\}$ is small, with a maximum value of $\approx 9.4\%$. The maximum value was obtained for $D_{throat} = 30\mu m$, which again reaffirms the results obtained in thrust and mass flow rate percentage differences, that the application of slip formulations only makes sense for conical nozzles having $D_{throat} < 30\mu m$.

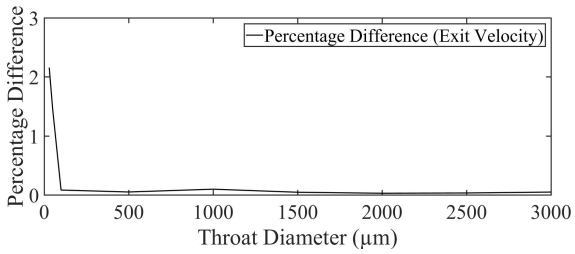

FIG. 15. Conical Nozzle : Exhaust Velocity percentage difference

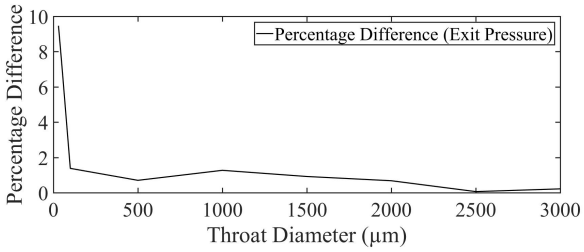

FIG. 16. Conical Nozzle : Exit pressure percentage difference

B. Bell Nozzle

A similar comparison between the thrust, exit pressure, exit velocity, and mass flow rate under the slip and no-slip treatments was carried out. The results are as shown:

1. Thrust : Percentage Difference

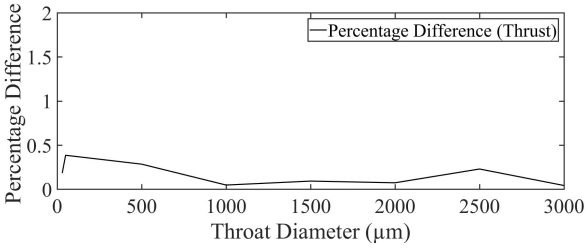

FIG. 17. Bell Nozzle : Thrust percentage difference

Figure 17 shows the percentage difference of thrust obtained for nozzles of different D_{throat} values. It was observed

that for all the simulations, irrespective of the D_{throat} values, the percentage difference between the slip and no-slip treatment was $< 0.5\%$. This indicates that, for bell nozzles, no-slip formulations can be used even for smaller D_{throat} values. This may be attributed to the fact, that in bell nozzles the expansion of the exhaust is not as rapid as in conical nozzles, this results in lower values of velocity gradients and hence smaller values of wall slip velocities and temperature discontinuity.

2. *Mass Flow Rate : Percentage Difference*

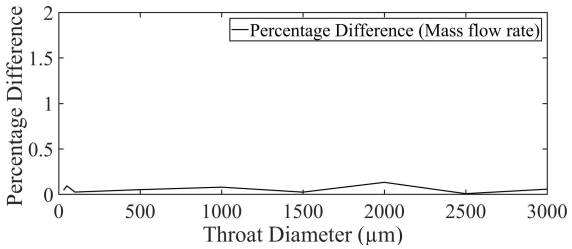

FIG. 18. Bell Nozzle : Mass flow rate percentage difference

Next, the percentage difference in the mass flow rate from the conical nozzles was compared under the effects of the slip and no-slip formulations. It can be seen in Figure 18. A similar trend was observed and the percentage difference across all the D_{throat} values was $< 0.2\%$.

3. *Exit Pressure : Percentage Difference*

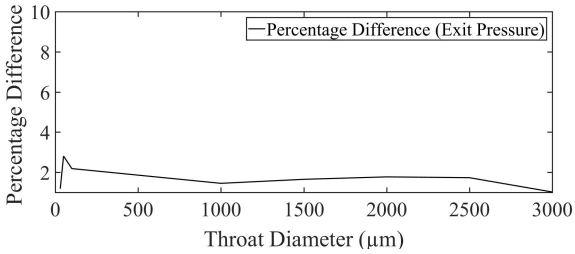

FIG. 19. Bell Nozzle : Exit Pressure percentage difference

Furthermore, from Figure 19, the percentage difference in the exit pressure was observed and, it was seen that no significant change across the all the D_{throat} values occurred. The maximum percentage difference observed was $< 3\%$.

4. *Exhaust Velocity : Percentage Difference*

Finally the same analysis was done for the exhaust velocity (in Figure 20). It was seen that, there was no significant change in average exhaust velocity between the slip and no- slip treatments. The maximum percentage difference was $< 0.5\%$.

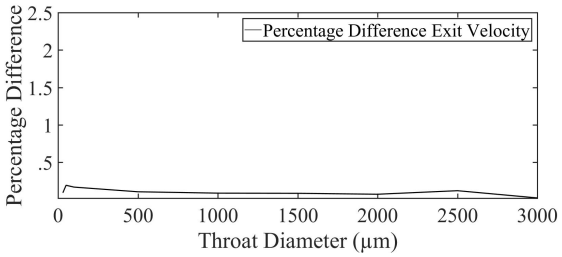

FIG. 20. Bell Nozzle : Exhaust velocity percentage difference

IX. CONTOUR PLOTS

In this section, contour plots for velocity, static temperature, Reynolds number and Knudsen number are shown for conical and bell nozzles with $D_{throat} = 50\mu m$. The difference between the properties as calculated by slip and no-slip formulations is very small and is not discernible from the contour plots. Figure 21-26 illustrate the flow contours for the aforementioned properties, it is evident that these contours cannot be used to distinguish between the slip and no-slip treatments. However, they shed some light on the general flow behavior in micro-nozzles. It can be seen that the viscous sub-layer extends well into the nozzles and occupies a sizable fraction of their volume.

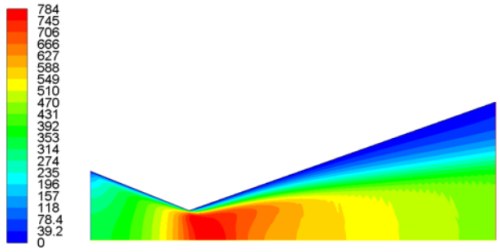

FIG. 21. Conical Nozzle : No-Slip Reynolds Number

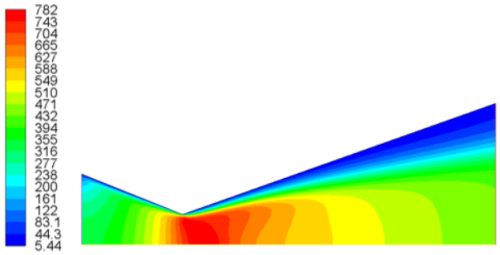

FIG. 22. Conical Nozzle : Slip Reynolds Number

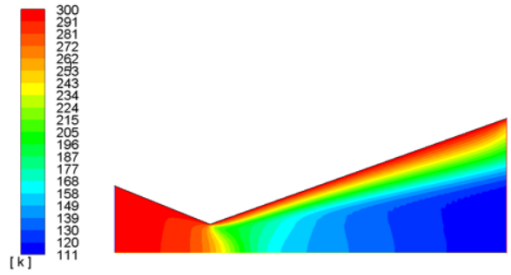

FIG. 23. Conical Nozzle : No-Slip Static Temperature

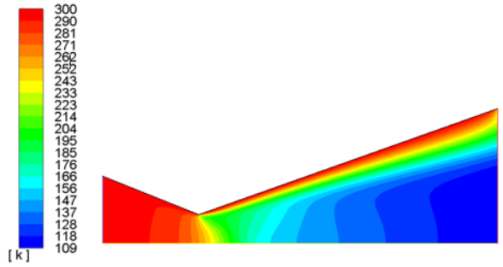

FIG. 24. Conical Nozzle : Slip Static Temperature

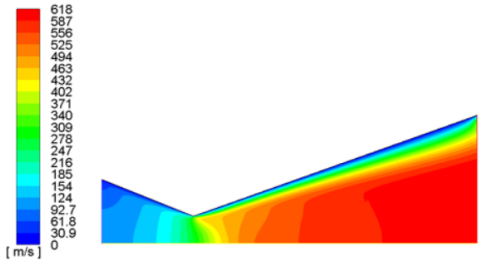

FIG. 25. Conical Nozzle : No-Slip Velocity Magnitude

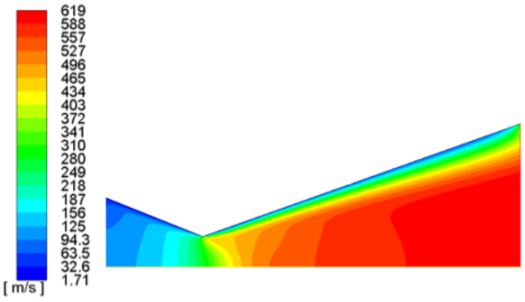

FIG. 26. Conical Nozzle : Slip Velocity Magnitude

A. Maximum Knudsen Number

The Knudsen Number contours for these nozzles are shown in Figure 27-28 , it can be seen that the Knudsen number indicates a necessity for the application of slip models at the walls. However, application of slip models does not depict much difference in nozzle performance characteristics (like thrust, exit pressure etc).

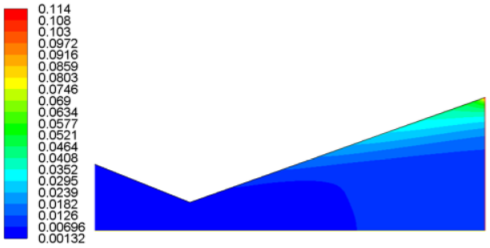

FIG. 27. Conical Nozzle : Knudsen Number

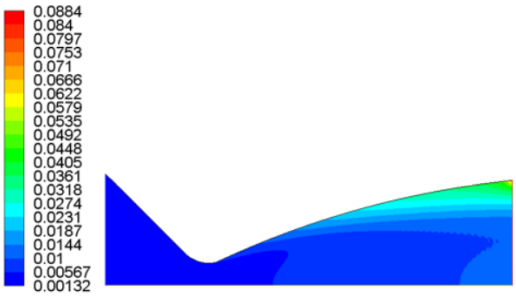

FIG. 28. Bell Nozzle : Knudsen Number

X. CONCLUSION

In this paper, the application of slip boundary condition to micro-nozzle walls is explored in detail, the results of the wall slip velocity and temperature jump for nozzles of D_{throat} ranging from $30\mu m$ to $40000\mu m$ are plotted and critically analysed. Furthermore, the difference between the slip treatment and the no-slip treatment for the nozzles is carried out. The difference in the properties of the nozzles is studied under these treatments and the results have been analysed. It is hypothesized that the magnitude of wall slip and temperature discontinuity increases at locations where the flow experiences rapid expansion, this is an important point that should be considered during the design of micro-nozzles. Furthermore, it was found that the wall-slip velocity and temperature discontinuity is lower in bell nozzles than in conical nozzles. Furthermore, it is also found that the application of special wall boundary conditions like the first order formulation is not necessary for the range of nozzles studied, however it is also seen that as the physical dimensions of the nozzles decrease further, the percentage difference of parameters like thrust, pressure, velocity and mass-flow rate show a rapid spike. This indicates that, special formulations are required for nozzle diameters $< 30\mu m$ in case of conical nozzles. Furthermore, it was found that in although, in many cases, the maximum Knudsen number reached in the flow indicated a necessity for the application of slip models, there was not much difference in nozzle characteristics when evaluated through purely continuum or partial-slip models. This indicates that the choice of the computational model is not completely based on the Knudsen number.

XI. REFERENCES

1. Banazadeh, A., & Gol, H. A. (2012). *Multi-objective trade-off analysis of an integrated cold gas propulsion system.* Proceedings of the Institution of Mechanical Engineers, Part G: Journal of Aerospace Engineering, 227(8), 1233-1250. doi:10.1177/09544
10012452234

2. Bayt, R., Ayon, A., Breuer, K., Bayt, R., Ayon, A., & Breuer, K. (1997). *A performance evaluation of MEMS-based micronozzles. 33rd Joint Propulsion Conference and Exhibit.* doi:10.2514/6.1997-3169

3. Das, T. R., Reed, C. O., & Eubank, P. T. (1973). *PVT [pressure-volume-temperature] surface and thermodynamic properties of butane.* Journal of Chemical & Engineering Data, 18(3), 244-253. doi:10.1021/je60058a002

4. Gibbon, D., Underwood, C., Sweeting, M., & Amri, R. (2002). *Cost effective propulsion systems for small satellites using butane propellant.* Acta Astronautica, 51(1-9), 145-152. doi:10.1016/s0094-5765(02)00074-7

5. Grm, A., Grönland, T., & Rodič, T. (2011). *Numerical analysis of a miniaturised cold gas thruster for micro- and nano-satellites.* Engineering Computations, 28(2), 184-195. doi:10.1108/02644401111109222

6. Groll, R. (2014). *Micro diffuser flow modeling for cold gas propulsion systems.* Pamm, 14(1), 633-640. doi:10.1002/pamm.201410304

7. Huzel, D. K. (1992). *Modern Engineering for Design of Liquid-Propellant Rocket Engines*. AIAA.

8. Louisos, W., Alexeenko, A., Hitt, D., & Zilic, A. (2008). *Design considerations for supersonic micronozzles.* International Journal of Manufacturing Research, 3(1), 80. doi:10.1504/ijmr.2008.016453

9. Ranjan, R., Chou, S. K., Riaz, F., & Karthikeyan, K. (2017). *Cold gas micro propulsion development for satellite application.* Energy Procedia, 143, 754-761. doi:10.1016/j.egypro.2017.12.758

10. Xie, C. (2007). *Characteristics of micronozzle gas flows. Physics of Fluids*, 19(3), 037102. doi:10.1063/1.2709707

11. Masoud Darbandi, Ehsan Roohi. *Study of subsonic / supersonic gas flow through micro/nanoscale nozzles using unstructured DSMC solver*. Microfluid Nanofluid (2011) 10, 321-335 doi: 10.1007/s10404-010-0671-7